The fusing ability of sperm is bestowed by CD9-containing vesicles released from eggs in mice

Kenji Miyado*[†‡§], Keiichi Yoshida[‡¶], Kazuo Yamagata[‖], Keiichi Sakakibara*, Masaru Okabe**, Xiaobiao Wang*, Kiyoko Miyamoto*, Hidenori Akutsu*, Takahiko Kondo*, Yuji Takahashi*, Tadanobu Ban[††], Chizuru Ito[¶], Kiyotaka Toshimori[¶], Akihiro Nakamura*, Masahiko Ito*, Mami Miyado*, Eisuke Mekada**, and Akihiro Umezawa*

*National Center for Child Health and Development, 2-10-1 Okura, Setagaya, Tokyo 157-8535, Japan; [†]School of Biomedical Science, Tokyo Medical and Dental University, Yushima, Bunkyo, Tokyo 113-8510, Japan; [¶]Graduate School of Medicine, Chiba University, 1-8-1 Inohana, Chuo-ku, Chiba 260-8670, Japan; [‖]Center for Developmental Biology, RIKEN Kobe Institute, 2-2-3 Minatojima-minamimachi, Chuo-ku, Kobe, Hyogo 650-0047, Japan; and **Research Institute for Microbial Diseases, and [††]Faculty of Medicine, Osaka University, 3-1 Yamadaoka, Suita, Osaka 565-0871, Japan

Edited by Ryuzo Yanagimachi, University of Hawaii, Honolulu, HI, and approved July 8, 2008 (received for review November 8, 2007)

Membrane fusion is an essential step in the encounter of two nuclei from sex cells—sperm and egg—in fertilization. However, aside from the involvement of two molecules, CD9 and Izumo, the mechanism of fusion remains unclear. Here, we show that sperm–egg fusion is mediated by vesicles containing CD9 that are released from the egg and interact with sperm. We demonstrate that the $CD9^{-/-}$ eggs, which have a defective sperm-fusing ability, have impaired release of CD9-containing vesicles. We investigate the fusion-facilitating activity of CD9-containing vesicles by examining the fusion of sperm to $CD9^{-/-}$ eggs with the aid of exogenous CD9-containing vesicles. Moreover, we show, by examining the fusion of sperm to $CD9^{-/-}$ eggs, that hamster eggs have a similar fusing ability as mouse eggs. The CD9-containing vesicle release from unfertilized eggs provides insight into the mechanism required for fusion with sperm.

fertilization | membrane fusion | EGFP | exosome

Fertilization is an essential process that naturally produces a cell capable of developing into a new individual. It consists of sequential events, including membrane fusion of sperm and egg (1). Despite the importance of understanding fertilization in controlling human reproduction and preserving endangered species, the molecular basis underlying the fusion remains a mystery, however. Previously, we reported that a tetraspan-membrane protein (tetraspanin), CD9, is expressed on the egg plasma membrane and is required for sperm–egg fusion (2–4). A role of CD9 in other fusion events also has been demonstrated (5). When sperm are added to eggs from $CD9^{-/-}$ females, the sperm bind to the egg plasma membrane normally, but fusion is severely impaired (2–4). Two recent observations suggest that CD9 plays a role in the organization of egg membrane. First, CD9 is transferred from the egg to the fertilizing sperm present in the perivitelline space (PVS) (6), suggesting the involvement of a process similar to trogocytosis, a mechanism of cell-to-cell contact-dependent transfer of membrane fragments (7). Second, CD9 deficiency alters the length and density of microvilli on the egg plasma membrane (8). CD9 is also known to be a component of exosomes, membrane vesicles released from a wide range of cells (9, 10). Despite its relationship to CD9, the involvement of exosome release in sperm–egg fusion remains unknown. In the present study, we analyzed the potential of enhanced green fluorescent protein (EGFP)-tagged CD9 (CD9-EGFP) as a reporter protein to study sperm–egg fusion in living mouse eggs.

Results

To observe the movement of CD9 during sperm–egg fusion, we generated a transgenic mouse line that expressed CD9-EGFP only in eggs (Fig. 1*A*), and converted to the genetic background of $CD9^{-/-}$ mice by mating mice. Western blot analysis using anti-CD9 monoclonal antibody (mAb) revealed that an expected CD9-EGFP with a molecular mass of 51 kDa (CD9 and EGFP contributing to 24 and 27 kDa, respectively) was expressed in the eggs collected from $Tg^{+}CD9^{-/-}$ mice; however, the amount of CD9-EGFP expressed in $CD9^{-/-}$ eggs was estimated to be 10% of that of endogenous CD9 in the $CD9^{+/+}$ eggs (Fig. 1*B*). Despite the small amount of CD9-EGFP expressed in eggs, CD9-EGFP demonstrated the ability to reverse the sterility of $CD9^{-/-}$ females (Fig. 1*C*). The numbers of pups obtained from $Tg^{+}CD9^{-/-}$ females (6.4 ± 0.5) were similar to those from

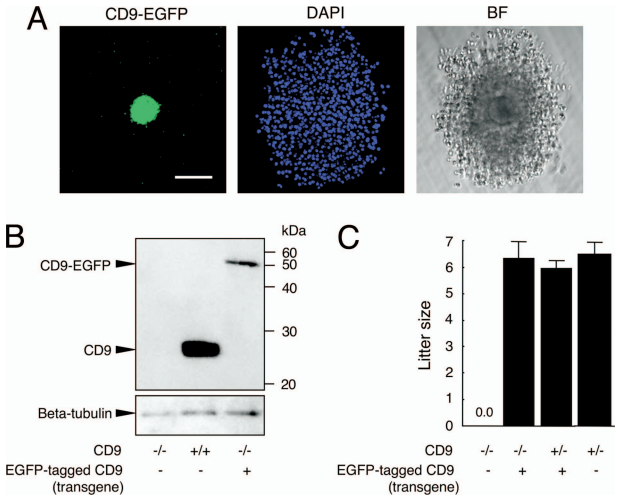

Fig. 1. Generation of mice expressing CD9-EGFP in eggs. (*A*) CD9-EGFP specifically expressed in eggs with mouse ZP3-promoter. Cumulus oocyte complex from $Tg^{+}CD9^{+/+}$ oviducts was collected at 14 h after injection of human chorionic gonadotropin. Nuclei of an egg and cumulus cells were counterstained with DAPI. (*Left*) CD9-EGFP. (*Center*) DAPI. (*Right*) Bright field. Scale bar: 100 μm. (*B*) Western blot analysis for eggs collected from $CD9^{-/-}$, $CD9^{+/+}$, and $Tg^{+}CD9^{-/-}$ mice. The same amounts, including 30 eggs of each lysate, were examined by anti-CD9 and anti-beta-tubulin mAbs (internal control). (*C*) Litter sizes of $CD9^{-/-}$ ($n = 31$), $Tg^{+}CD9^{-/-}$ ($n = 35$), $Tg^{+}CD9^{+/-}$ ($n = 16$), and $CD9^{+/-}$ mice ($n = 15$) (mean ± SEM). The numbers of females examined are in parentheses.

Author contributions: K. Miyado, K. Yamagata, M.O., and A.U. designed research; K. Miyado, K. Yoshida, K.S., X.W., K. Miyamoto, H.A., T.K., Y.T., T.B., C.I., A.N., M.I., and M.M. performed research; K. Miyado contributed new reagents/analytic tools; K. Miyado, K. Yoshida, H.A., K.T., E.M., and A.U. analyzed data; and K. Miyado wrote the paper.

The authors declare no conflicts of interest.

This article is a PNAS Direct Submission.

Freely available online through the PNAS open access option.

[‡]K. Miyado and K. Yoshida contributed equally to this work.

[§]To whom correspondence should be addressed. E-mail: kmiyado@nch.go.jp.

This article contains supporting information online at www.pnas.org/cgi/content/full/0710608105/DCSupplemental.

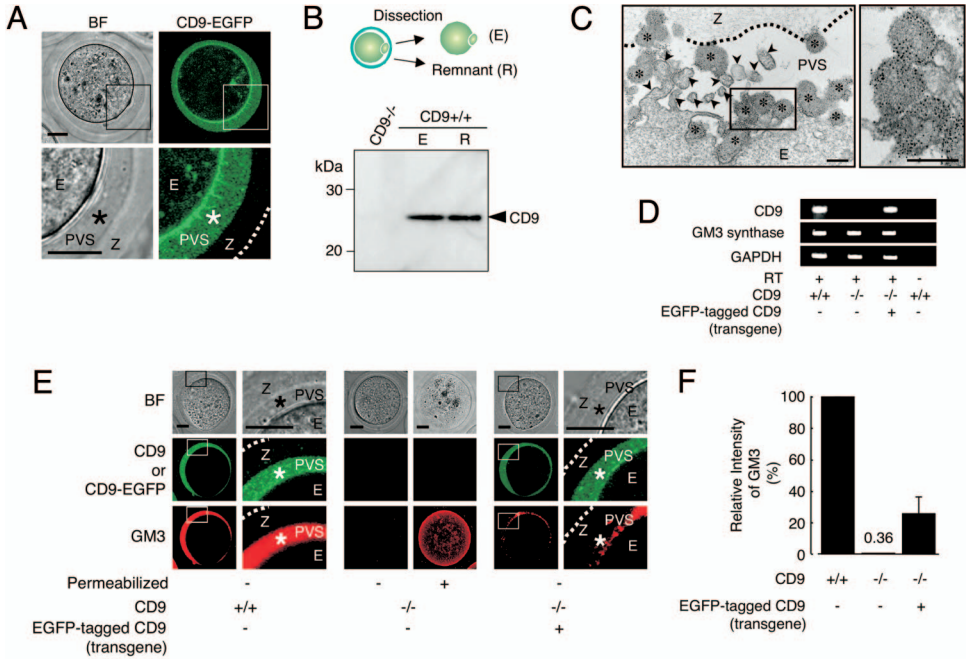

Fig. 2. Identification of secretory vesicles containing CD9 from unfertilized eggs. *A*, A single confocal image showing CD9-EGFP in unfertilized $Tg^{+}CD9^{-/-}$ eggs (E), including the PVS (*), zona pellucida (Z), and the outer margin of the zona pellucida (dotted line). (*Left*) Bright field. (*Right*) CD9-EGFP. *Lower* are enlarged images of the boxed areas. (*B*) Western blot analysis for eggs mechanically fractionated as shown in the diagram: zona-intact $CD9^{-/-}$ eggs (E) (10 eggs per lane) and zona-free $CD9^{+/+}$ eggs (10 eggs per lane). The medium (R) containing the remnant material from 40 eggs treated with a piezo manipulator was loaded in each lane. (*C*) Immunoelectron-microscopic analysis of $CD9^{+/+}$ eggs. The zona-intact $CD9^{+/+}$ eggs were examined using anti-CD9-mAb and 5-nm gold beads conjugated with anti-rat IgG Ab. Left panel: Image including CD9-containing vesicles (*), microvilli (arrowheads), zona pellucida (Z), perivitelline space (PVS), and egg (E). (*Right*) An enlarged image of the boxed region in the left panel. Scale bar: 200 nm. (*D*) RT-PCR for CD9, GM3 synthase, and glyceraldehyde-3-phosphate dehydrogenase transcripts in $CD9^{+/+}$, $CD9^{-/-}$, and $Tg^{+}CD9^{-/-}$ eggs. The same amounts, including 50 eggs in each reaction, were examined. The right end lanes are negative controls in which RT was removed from reactions of wild-type eggs. (*E*) Localization of GM3 and CD9 in $CD9^{+/+}$, $CD9^{-/-}$, and $Tg^{+}CD9^{-/-}$ eggs. (*Left*) Wild-type. (*Middle*) $CD9^{-/-}$. (*Right*) $Tg^{+}CD9^{-/-}$. Right-side of the sets of wild-type and $Tg^{+}CD9^{-/-}$ eggs are enlarged images of the boxed regions. The live eggs were examined, and the internal localization of GM3 in $CD9^{-/-}$ eggs was examined under fixed, permeabilized conditions. (*F*) Comparison of the fluorescent intensities of GM3 stained by antibody in wild-type ($n = 10$), $CD9^{-/-}$ ($n = 9$), and $Tg^{+}CD9^{-/-}$ eggs ($n = 10$) (mean ± SEM). The average values of the wild-type eggs were set to 100%.

$Tg^{+}CD9^{+/-}$ and $CD9^{+/-}$ females (6.0 ± 0.2 and 6.5 ± 0.5) and greater than those from $CD9^{-/-}$ females (0.0 ± 0.0). The $CD9^{+/-}$ females did not exhibit any loss in fertility that could cause a reduction of litter size relative to that of the $CD9^{+/+}$ females (4). Furthermore, the transgene had no effect on normal fertility. These results demonstrate that transgenically expressed CD9-EGFP can compensate for the loss of intrinsic CD9 and yield eggs with the ability to fuse with sperm.

Based on the foregoing evidence, we observed the subcellular localization of CD9-EGFP in "living" $Tg^{+}CD9^{-/-}$ eggs (Fig. 2*A*). As expected, confocal microscopic analysis allowed the visualization of two types of CD9-EGFP localization: intense on the plasma membrane and also in the cytoplasm. Unexpectedly, we found loosely filled, noncompacted CD9-EGFP in the PVS, a space formed between the zona pellucida and the plasma membrane of the egg. The localization of CD9 outside the eggs also was confirmed by Western blot analysis using anti-CD9 mAb (Fig. 2*B*). As shown in the diagram, $CD9^{+/+}$ eggs were mechanically fractionated into denuded eggs and other components (R) using a piezo manipulator (11). The fraction R, containing the zona pellucida and the components in the PVS, was centrifuged and subjected to Western blot analysis. The amount of CD9 in the remnant material from 40 eggs was found to be densitometrically equal to that of 10 zona-free eggs, demonstrating an estimated relative abundance of CD9 in the remnant of 20% per egg. Subsequently, we performed immunoelectron-microscopic analysis on the $CD9^{+/+}$ eggs. We identified the vesicles bound to gold particles inside the PVS (Fig. 2*C*). The sectioned microvilli contained a branched network of actin filaments, whereas the variously sized vesicles (50–250 nm in diameter) had uniformly dense materials rather than actin filaments. We also compared $CD9^{+/+}$, $Tg^{+}CD9^{-/-}$, and $CD9^{-/-}$ eggs by electron-microscopic analysis [supporting information (SI) Fig. S1]. The accumulation of vesicles in the PVS in the $Tg^{+}CD9^{-/-}$ eggs was comparable to that in the $CD9^{+/+}$ eggs, whereas it was not seen in the $CD9^{-/-}$ or germinal vesicle-staged $CD9^{+/+}$ eggs. These results indicate that 20% of the total amount of CD9 is stored as vesicles in the PVS during meiosis.

We next examined the expression of ganglioside GM3, identified as a CD9-associated molecule (12) and a component of exosomes (10), in $CD9^{+/+}$, $CD9^{-/-}$, and $Tg^{+}CD9^{-/-}$ eggs. First, we confirmed the expression of GM3 synthase (ST3GalV/SAT-1) (13) in these eggs by RT-PCR (Fig. 2*D*). Then we investigated the localization of GM3 by immunostaining these live eggs with anti-GM3 mAb (Fig. 2*E*). This antibody has been demonstrated to recognize GM3 in the plasma membrane of cells without treatment for permeabilization (14). Finally, we measured the fluorescent intensities of GM3 in these live eggs (Fig. 2*F*). As expected, in wild-type eggs, GM3 was colocalized with CD9 in the PVS and plasma membrane (Fig. 2*E Left* and Fig. 2*F*). In contrast, in $CD9^{-/-}$ eggs, the fluorescent intensities of GM3 were decreased dramatically in the PVS and plasma membrane (0.4% ± 0.2%, relative to 100% for the $CD9^{+/+}$ eggs), consistent with the loss of CD9 (Fig. 2*E Center* and Fig. 2*F*), whereas GM3 could be detected in the cytoplasm of $CD9^{-/-}$ eggs that had been permeabilized by a detergent after fixation. Moreover, the expression of CD9-EGFP reversed the decrease of GM3 in the PVS and plasma membrane of $CD9^{-/-}$ eggs (25.6 ± 10.7%) (Fig. 2*E Right* and Fig. 2*F*), corresponding to the amount of CD9-EGFP quantified by Western blot analysis (Fig. 1*B*). In addition, electron-microscopic analysis revealed that the number of characteristic membrane structures, termed microvilli (1), were significantly decreased in the $CD9^{-/-}$ eggs compared with the $CD9^{+/+}$ eggs (Fig. S2 *A* and *B*). The numbers of microvilli were increased by ≈50% by the expression of CD9-EGFP in the $CD9^{-/-}$ eggs. The analyses of three types of eggs indicate that CD9- and GM3-containing vesicle release is linked to microvilli formation.

We next investigated the involvement of CD9-containing vesicles in sperm–egg fusion (Fig. 3). We found that, based on the length of microvilli (Fig. S2*C*), zona-intact $Tg^{+}CD9^{-/-}$ eggs can be categorized into two groups (Fig. 3*A*). From single

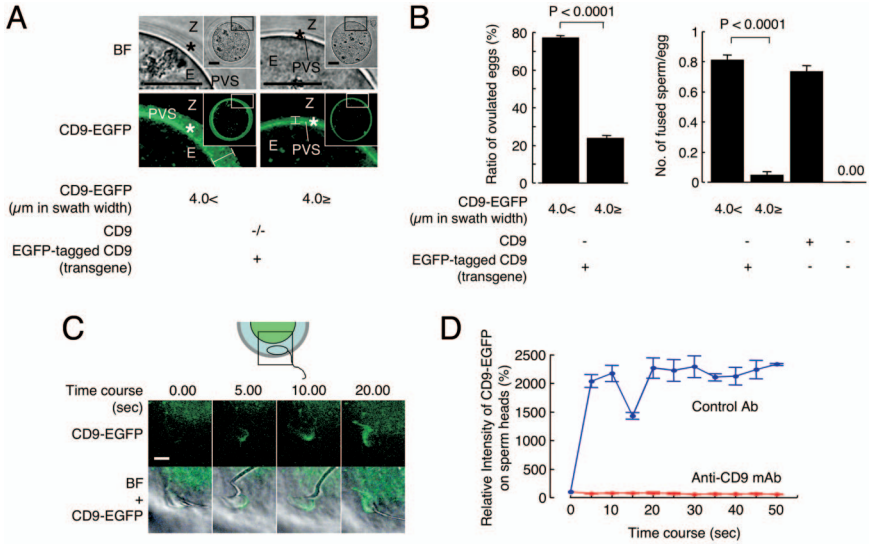

Fig. 3. Involvement of CD9-containing vesicles in sperm–egg fusion. (*A*) Categorization of $Tg^{+}CD9^{-/-}$ eggs (E) into two groups according to the thickness of CD9-EGFP in the PVS (*) and the inner region of the zona pellucida (Z) (>4.0 μm or ≤ 4.0 μm), indicated by double-headed lines. The boxed regions in *Insets* are enlarged. Scale bar: 20 μm. (*B*) Comparison of the fusing ability of two groups of $Tg^{+}CD9^{-/-}$ eggs with wild-type sperm. Left graph: Ratio of two groups of $Tg^{+}CD9^{-/-}$ eggs ovulated from 12 females (mean ± SEM). Right graph: Number of sperm fused per egg in two groups of zona-intact $Tg^{+}CD9^{-/-}$ eggs ovulated from 12 females (>4.0 μm, $n = 204$; ≤4.0 μm, $n = 66$) (mean ± SEM). $CD9^{+/+}$ ($n = 120$) and $CD9^{-/-}$ ($n = 112$) served as positive and negative controls, respectively. (*C* and *D*) Monitoring of the association of egg CD9-containing vesicles with wild-type sperm. $Tg^{+}CD9^{-/-}$ eggs were incubated with the sperm and monitored immediately after the sperm penetrated the zona pellucida under the presence of anti-CD9 mAb (boxed region). The values were calculated from data scanning by confocal microscopy (15 sperm in triplicate dishes) Blue: Preimmune rat IgG. Red: Anti-CD9 mAb (KMC8) (mean ± SEM). The average values of the fluorescent intensities of CD9-EGFP at 0 s were set to 100%, and the final concentration of antibodies was adjusted to 50 μg/ml. Scale bar, 5 μm.

confocal images sectioned through the largest diameter, the accumulation of CD9-EGFP from the plasma membrane to the inner region of the zona pellucida was >4.0 μm in swath width in one group and ≤ 4.0 μm in the other group. The accumulation of CD9-EGFP was predicted to show that CD9-containing vesicles are more highly accumulated within the PVS in the >4.0-μm group compared with the ≤ 4.0-μm group. Comparing the ratio of these two groups in $Tg^{+}CD9^{-/-}$-ovulated eggs revealed a much higher percentage of the >4.0-μm group (77.0 ± 1.3% vs.23.7 ± 1.5%) (Fig. 3*B Left*). Therefore, we focused on the heterogeneity of CD9-EGFP accumulation within the PVS and determined the ratio of the two groups in zona-intact $Tg^{+}CD9^{-/-}$ eggs that successfully fused with the sperm 6 h after insemination. The >4.0-μm group of $Tg^{+}CD9^{-/-}$ eggs showed higher activity for fusion with sperm (0.81 ± 0.04 sperm fused per egg), compared with the ≤40-μm group of $Tg^{+}CD9^{-/-}$ eggs (0.05 ± 0.03) and the $CD9^{-/-}$ eggs (0.00 ± 0.00), and comparable activity to that of wild-type eggs (0.73 ± 0.04) (Fig. 3*B Right*). The average activity of all $Tg^{+}CD9^{-/-}$ eggs (0.72 ± 0.03 sperm fused per egg) was equal to that of wild-type eggs (0.73 ± 0.04 sperm fused per egg). The difference between the two groups of $Tg^{+}CD9^{-/-}$ eggs was statistically significant (Fig. 3*B*). These results suggest that the quantities of CD9-containing vesicles, as assessed by the swath width of CD9-EGFP, are strongly correlated with the frequency of sperm–egg fusion.

To detect the association between sperm and CD9-containing vesicles, we serially monitored the wild-type sperm that penetrated the zona pellucida of the $Tg^{+}CD9^{-/-}$ eggs (Fig. 3 *C* and *D*). As shown in the diagram, we began monitoring the sperm immediately after the head portion of sperm penetrated the zona pellucida of the $Tg^{+}CD9^{-/-}$ eggs (Fig. 3*C Upper*, boxed area in the diagram). Soon after we began to monitor the sperm, the fluorescent intensities of CD9-EGFP on the sperm heads increased and then decreased rapidly between 0 s and 15 s, then increased again, reaching a maximum at 20 s. At this point, the CD9-EGFP fully covered the surface of the sperm heads. In contrast, when the sperm were incubated with $Tg^{+}CD9^{-/-}$ eggs in the medium containing anti-CD9 mAb, no increase in intensity of CD9-EGFP on the sperm heads was detected. Anti-CD9 mAbs have been reported to inhibit sperm–egg fusion (4, 15, 16). Our findings demonstrate that the anti-CD9 mAb inhibited the association of sperm with CD9-containing vesicles in parallel to inhibition of sperm–egg fusion.

To determine whether CD9-containing vesicles are capable of initiating sperm–egg fusion, we incubated the sperm with $CD9^{-/-}$ eggs in medium containing the vesicles collected from $CD9^{+/+}$ eggs (Fig. 4 and Fig. S3). To restrict the source of CD9 into the vesicles from the $CD9^{+/+}$ eggs, we used sperm collected from the epididymis of $CD9^{-/-}$ males. We estimated the capability of the vesicles to influence fusion by counting the number of sperm fused with $CD9^{-/-}$ eggs. As shown in the experimental design, after the zona pellucida was removed from the $CD9^{-/-}$ eggs, the eggs were incubated with sperm in the medium containing the vesicles (Fig. 4*A*). When examined at 1 h after incubation, the sperm were seen to be capable of fusing with $CD9^{-/-}$ eggs after co-incubation with the vesicles (Fig. 4*A Center*), indicating restoration of the fusibility of $CD9^{-/-}$ eggs with the sperm (0.58 ± 0.07 sperm fused per egg) (Fig. 4*B*). We detected further evidence of sperm–egg fusion in the $CD9^{-/-}$ eggs from which a second polar body had been extruded. In contrast, we did not detect improved fusibility of sperm with eggs in medium depleted of CD9-containing vesicles using beads conjugated with anti-CD9 mAb (Fig. 4*A Right* and *B*). After treatment with the beads, the quantity of CD9 in the depleted medium was significantly decreased, to 16% of the untreated medium (Fig. 4*C*). In addition, $CD9^{-/-}$ remnants failed to rescue the fusing ability of $CD9^{-/-}$ eggs. These findings indicate that the association with CD9-containing vesicles renders the sperm capable of fusing with eggs without endogenous CD9 expression. We estimated the relative abundance of CD9 in the remnant as 18% of the total amount in the eggs (Fig. 4*C*). We further found

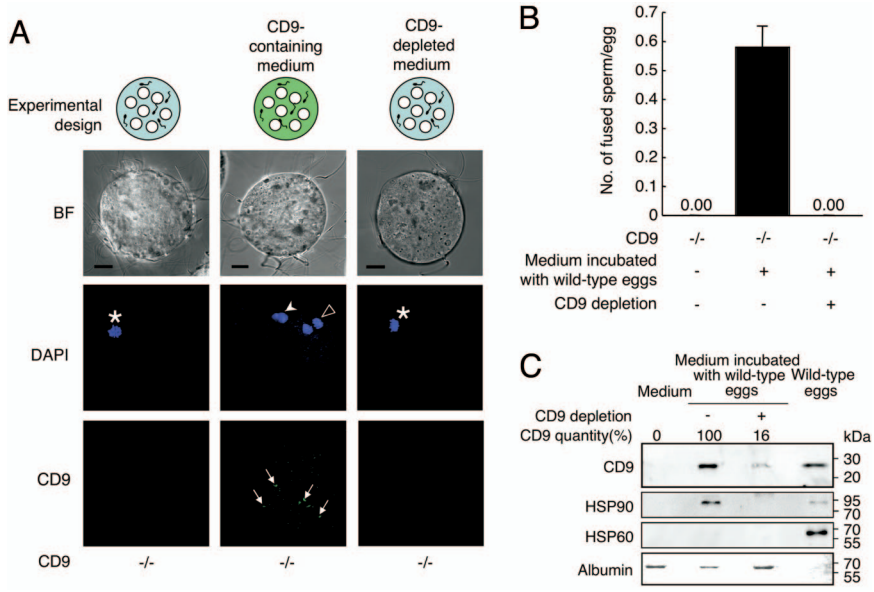

Fig. 4. Identification of fusion-facilitating activity of CD9-containing vesicles. (*A*) Estimation of the fusion-facilitating ability of the vesicles in sperm–egg fusion. As shown in the experimental design, $CD9^{-/-}$ sperm were incubated with $CD9^{-/-}$ eggs (white circles) in media containing egg-released vesicles after the zona pellucida was removed from these eggs. CD9 was detected by anti-CD9 mAb conjugated with Alexa488. The eggs were preloaded with DAPI before incubation with the sperm, to allow counting of the number of fused sperm. (*Left*) $CD9^{-/-}$ eggs at 1 h after incubation with the sperm, as a negative control. *Center* $CD9^{-/-}$ eggs cultured in the medium containing CD9 collected from wild-type eggs. (*Right*) $CD9^{-/-}$ eggs cultured in the medium depleted of CD9 by beads conjugated with anti-CD9 mAb, showing the fused sperm to eggs (arrowhead), metaphase II–arrested chromosomes (*), a second polar body (open arrowhead), and CD9 translocated on the sperm heads (arrow). The fluorescent z-series images were projected as three-dimensional images. Scale bar: 20 μm. (*B*) Number of fused sperm with the zona-free eggs counted at 1 h after incubation (mean ± SEM): $CD9^{-/-}$ eggs as a negative control ($n = 51$), $CD9^{-/-}$ eggs cultured in the medium containing CD9 ($n = 112$), and $CD9^{-/-}$ eggs cultured in the medium depleted of CD9 by antibody-conjugated beads ($n = 74$). The total numbers of eggs examined are in parentheses. (*C*) Western blot analysis of the media incubated with $CD9^{+/+}$ eggs for CD9, HSP90, and HSP60. Loaded samples (left to right): The medium as a negative control, the medium containing the remnant material from 40 eggs per lane (bead-untreated and -treated), and 5 eggs per lane as a positive control. The albumin contained in the medium was detected by Coomassie brilliant blue staining as an internal control. The quantities of CD9 in the media were measured densitometrically (using National Institutes of Health Image software).

that the decreased amount of CD9 after the bead treatment was synchronized with that of a cytoplasmic chaperone, HSP90 (17), but not with a mitochondrial chaperone, HSP60 (18). Our analysis of the egg-conditioned medium indicated that CD9-containing vesicles contained HSP90, a conserved component of exosomes (9, 10).

To estimate the contribution of CD9-containing vesicles to sperm–egg fusion, we examined the restoration of the impaired sperm-fusing ability in $CD9^{-/-}$ eggs co-incubated with $CD9^{+/-}$ or $CD9^{+/+}$ eggs expressing endogenous CD9 (Figs. 5 and S4*A*). We predicted that when sperm were incubated with a mixture of eggs, the vesicles released from $CD9^{+/-}$ or $CD9^{+/+}$ eggs would

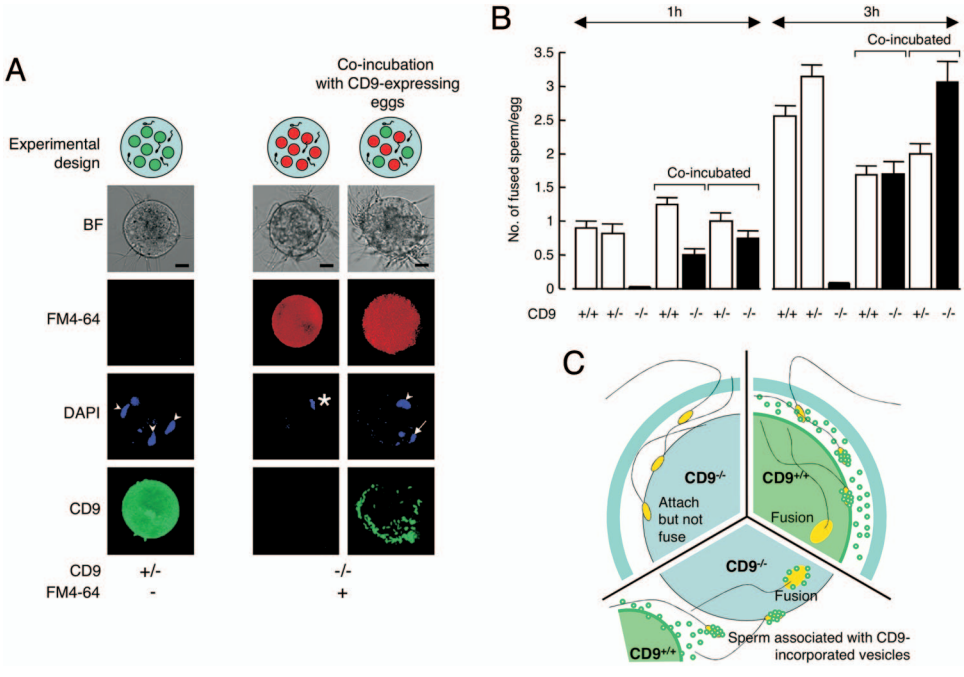

Fig. 5. Recovery of impaired fusion of $CD9^{-/-}$ eggs with sperm by CD9-containing vesicles. (*A*) Estimation of the fusion-facilitating ability of the vesicles in sperm–egg fusion. As shown in the experimental design, sperm were incubated with a mixture of CD9-expressing eggs (green circles) and $CD9^{-/-}$ eggs (red circles) after the zona pellucida was removed from these eggs. The eggs were preloaded with DAPI before incubation with sperm, to allow counting of the number of fused sperm. $CD9^{-/-}$ eggs were prestained with FM4–64 and thus were easily distinguished from CD9-expressing eggs after incubation with the sperm. (*Left*) $CD9^{+/-}$ eggs at 1 h after incubation with the sperm, as a positive control. (*Center*) $CD9^{-/-}$ eggs, as a negative control. (*Right*) $CD9^{-/-}$ eggs co-incubated with $CD9^{+/-}$ eggs, showing fused sperm to egg (arrowheads), metaphase II–arrested chromosomes (*), and extruded second polar body (arrow). The fluorescent z-series images were projected as three-dimensional images. CD9 was detected by anti-CD9 mAb conjugated with Alexa488. Scale bar: 20 μm. (*B*) Numbers of fused sperm with the zona-free eggs counted at 1 and 3 h after incubation (mean ± SEM). $CD9^{+/-}$ (1 h: $n = 34$; 3 h: $n = 55$), $CD9^{+/+}$ (1 h: $n = 71$; 3 h: $n = 79$), and $CD9^{-/-}$ eggs (1 h: $n = 100$; 3 h: $n = 115$) were separately incubated with sperm. Total number of coincubated eggs examined: $CD9^{+/-}$ eggs ($n = 54$) coincubated with $CD9^{-/-}$ eggs ($n = 60$), and $CD9^{+/+}$ eggs ($n = 65$) coincubated with $CD9^{-/-}$ eggs ($n = 74$) at 1 h; $CD9^{+/-}$ eggs ($n = 51$) coincubated with $CD9^{-/-}$ eggs ($n = 33$), and $CD9^{+/+}$ eggs ($n = 98$) coincubated with $CD9^{-/-}$ eggs ($n = 90$) at 3 h. (*C*) Schematic model of involvement of CD9-containing vesicles in sperm–egg fusion: $CD9^{+/+}$ (green), $CD9^{-/-}$ (light blue), and $CD9^{-/-}$ eggs coincubated with $CD9^{+/+}$ wild-type eggs with sperm (yellow).

interact with sperm, and these sperm could fuse with $CD9^{-/-}$ eggs. If sperm-fusing ability were regulated mainly by CD9-containing vesicles, then the number of sperm fused to $CD9^{-/-}$ eggs would be predicted to be almost equal to that fused to $CD9^{+/-}$ or $CD9^{+/+}$ eggs coincubated with $CD9^{-/-}$ eggs. We counted the number of fused sperm in coincubated CD9-expressing eggs ($CD9^{+/-}$ and $CD9^{+/+}$) and $CD9^{-/-}$ eggs. The $CD9^{-/-}$ eggs were prestained with FM4–64 (19), a fluorescent dye used to stain the membrane of live cells, and thus could be easily distinguished from the $CD9^{+/-}$ and $CD9^{+/+}$ eggs. FM4–64 did not transfer between the $CD9^{-/-}$ eggs and the $CD9^{+/-}$ or $CD9^{+/+}$ eggs. As shown in the experimental design, after the zona pellucida was removed from the eggs, $CD9^{-/-}$ eggs (red circles) were mixed with $CD9^{+/-}$ or $CD9^{+/+}$ eggs (green circles), and sperm were added to the medium containing these eggs (Fig. 5*A*). At 1 h after insemination, significant fusion of sperm with the $CD9^{-/-}$ eggs was facilitated (0.75 ± 0.11 and 0.50 ± 0.09 sperm fused per egg), corresponding to that in the $CD9^{+/-}$ (1.00 ± 0.13) and $CD9^{+/+}$ eggs (1.25 ± 0.10). At 3 h after insemination, the fusion of sperm with the $CD9^{-/-}$ eggs was restored (3.06 ± 0.30 and 1.70 ± 0.18 sperm fused per egg) to levels comparable to those in the $CD9^{+/-}$ (2.00 ± 0.15) and $CD9^{+/+}$ eggs (1.69 ± 0.13). We also detected a second polar body extruding from the $CD9^{-/-}$ eggs (Fig. 5*A Right*, arrow). In contrast, we did not observe the translocation of vesicles from the $CD9^{+/-}$ and $CD9^{+/+}$ eggs to the $CD9^{-/-}$ eggs when sperm were not added to the mixture, even after 10 h of incubation (Fig. S4*B*). These data demonstrate that the defect in the fusing ability of $CD9^{-/-}$ eggs is caused by dysfunction of the mechanism facilitating the sperm-fusing activity through CD9-containing vesicles.

To further study the involvement of CD9-containing vesicles in regulating sperm-fusing ability, we evaluated the capability of hamster eggs in sperm–egg fusion (Fig. S5). Hamster eggs have the ability to fuse with other mammalian sperm and thus are used as a tool to evaluate the fusing ability of human sperm (20). When hamster eggs were incubated with $CD9^{-/-}$ eggs after the zona pellucida was removed from these eggs, the sperm-fusing ability of these eggs was improved significantly. The sperm-fusing ability acquired through the exposure to hamster eggs was not as great as that produced by exposure to mouse eggs, probably due to the slightly different CD9 in hamster and mouse eggs (21). These results indicate that the function of CD9-containing vesicles in the acquisition of sperm-fusing ability is widely conserved in mammals.

Discussion

In sperm–egg fusion, there is a significant direct interaction between the cell membranes of sperm and eggs (1, 20, 22); however, our results demonstrate that CD9-containing vesicle–sperm interaction precedes the direct cell membrane interaction between sperm and eggs. Based on our data, we propose that the release of CD9-containing vesicles from eggs before fertilization facilitates the sperm-fusing ability that renders the sperm competent to fuse with $CD9^{-/-}$ eggs (Fig. 5*C*). Our finding of CD9-EGFP in living unfertilized eggs demonstrates that CD9-containing vesicles are present in the PVS, and that these vesicles accumulate inside the PVS during the germinal vesicle (1) and metaphase II-arrested stages (1). During this period, the egg undergoes drastic cytological changes with the increased number of microvilli (1, 22), predicting the correlation between vesicle release and microvilli formation. As expected, this correlation is supported by the finding that CD9 deficiency leads not only to impaired microvilli formation (8) (Fig. S2), but also to decreased accumulation of vesicles within the PVS. These data support the association between the release of CD9-containing vesicles from eggs and the formation of microvilli on the egg plasma membrane.

As reported previously, somatic cells are capable of releasing proteins and lipids included in membrane organelles, termed exosomes (9, 10), which are pinched out from the plasma membrane (23). Exosomes share many additional properties with retroviral particles, including similar lipid and protein compositions, such as tetraspanin (23). GM3 and HSP90 are known to be conserved components of exosomes (10). Our results show that CD9-containing vesicles released from eggs share these two components, implying that the vesicles are "exosome-like." Previous studies of macrophages have proposed that exosome biogenesis occurs only by outward budding at endosomal membranes, followed by the fusion of vesicle-laden endosomes with the plasma membrane (9, 23). If the CD9-containing vesicle were derived from exosomes and generated from the fusion of endosomes with the plasma membrane, then the vesicles would contain some proteases (9, 23), fuse with the sperm membrane, and possibly activate the sperm fusogenic factor(s) by enzymatic activities.

In hamster eggs, expansion of the PVS has been deemed essential or at least beneficial to normal fertilization (20, 21, 24), indicating that materials involved in fusion with sperm are released from eggs before fertilization in hamsters and in mice. Because anti-CD9 mAbs are not available for hamster CD9, we could not directly confirm CD9-containing vesicle release from hamster eggs before fertilization. Instead, our co-incubation assay demonstrated that hamster eggs facilitate the fusion of sperm with $CD9^{-/-}$ eggs, indicating that hamster eggs share a similar mechanism with mouse eggs through egg-released materials. Moreover, it has been reported that growing oocytes bind to sperm and transfer fluorescent dyes to the sperm head (25). At this stage, oocytes have CD9 on the cell membrane but lack CD9-containing vesicles (Fig. S1). We presume that the transfer of fluorescent dye from growing oocytes to sperm heads is mediated by CD9 on the cell membrane. Based on our findings, we propose that the CD9-containing vesicle has an ability to facilitate sperm—egg fusion. This knowledge has great potential for clinical applications, such as the induction of sperm–egg fusion using exogenous sources.

Materials and Methods

Animals. The mice that we produced were back-crossed into a C57BL/6 genetic background. Wild-type eggs were collected from C57BL/6 females (8–12 weeks old). Wild-type sperm were obtained from the epididymides of B6C3F1 males (8–12 weeks old). Hamster eggs were obtained commercially as frozen unfertilized eggs (NOSAN).

Antibodies and Chemicals. Antibodies against CD9 (KMC; BD PharMingen), beta-tubulin (Tub2.1; Sigma), HSP60 (24/HSP60; BD PharMingen), HSP90 (16F1; MBL), and GM3 (GMR6; Seikagaku) were used. Antibodies labeled with biotin by a labeling kit (Dojindo) and horseradish peroxidase-conjugated streptavidin (Sigma) were used for Western blot analysis. For immunostaining, antibodies were labeled directly with Alexa488 and Alexa546 using labeling kits (Invitrogen). FM4–64 (Invitrogen) was used to define the lipid bilayer of live eggs without disturbing sperm–egg fusion (10 μM at final concentration). We used DAPI (Invitrogen), a fluorescent dye that slowly permeates the living cell membrane (semipermeable) and slowly leaks out of cells after washing relative to Hoechst33342 (permeable), in counting the number of sperm fused per egg.

Transgenic Mice. The construct expressing mouse CD9 tagged at the N terminus with EGFP (CD9-EGFP) was subcloned into plasmid DNA-containing mouse ZP3 promoter (26). The expression cassette was excised by restriction enzyme digestion and microinjected into fertilized eggs of C57BL/6 mice, according to standard techniques (27).

Genotyping and RT-PCR. Mouse genotyping and RT-PCR were performed following standard procedures (27). (Primer sets are listed in Table S1).

Egg Collection. Eggs were collected from the oviduct 14–16 h after human chorionic gonadotropin injection (4). The eggs were placed in a drop of TYH

medium (28). Sperm collected from the epididymides were capacitated in a 100-μl drop of medium. The eggs were incubated with 1.5×10^5 sperm/ml at 37°C in 5% CO_2, and unbound sperm were washed away. The zona pellucida was removed from the eggs with acidic Tyrode's solution (4) or a piezo manipulator (11). A hole was punched through the zona pellucida with a piezo manipulator, and the eggs were removed. All materials were aspirated, including the medium but not the eggs, and used as ''remnants.''

Immunostaining. Zona-intact live eggs were stained with diluted antibodies in TYH medium for 30 min at 37°C, and the nonspecifically accumulated antibodies in the PVS were washed away after a brief incubation (30 min) in the medium. To measure the fluorescent intensities of GM3, three types of eggs were stained by Alexa546-labeled anti-GM3 mAb in TYH medium for 30 min, then washed in the medium for 30 min. Staining was visualized using a laser scanning confocal microscope (LSM 510 META; Carl Zeiss).

Electron-Microscopic Analysis. Live eggs were incubated with anti-CD9 mAb and anti-rat IgG mAb tagged with 5-nm gold beads. After incubation, the eggs were fixed by glutaraldehyde and osmic acid solutions. Ultra-thin sections were prepared as described in ref. 29. Eggs denuded with acid Tyrode's solution were fixed with a mixture of paraformaldehyde and glutaraldehyde and osmic acid solutions.

***In Vitro* Fertilization.** To observe the fusion with the sperm, zona-intact and zona-free eggs were incubated with DAPI (10 μg/ml) in the medium for 20 min, then washed before the sperm were added. This procedure allowed the staining of only fused sperm nuclei by dye-transfer into sperm after membrane fusion. At 1 h or 3 h after incubation in a 30-μl drop of medium, the eggs were fixed with a mixture of paraformaldehyde and glutaraldehyde for 20 min at 4°C.

Monitoring the Association of CD9-Containing Vesicles with Sperm. Eggs collected from $Tg^+CD9^{-/-}$ females were set in a 30-μl drop of TYM medium. The sperm were added to the eggs at a final concentration of 1.5×10^5/ml after incubation in the medium for 2 h. Posts of latex beads were deposited around the eggs. A glass coverslip was carefully pressed down onto the posts until the egg were fixed. The medium containing eggs and sperm was cooled to 10°C before observation. Cooling reduced the sperm motility. This procedure allowed us to measure the CD9-EGFP fluorescence on the sperm head using a confocal microscope. Images of the sperm were captured at 1 frame/s. The average value of the fluorescent intensities of CD9-EGFP at 0 s was set to 100%, and the final concentration of antibodies was adjusted to 50 μg/ml. The data are measurements of serial images from 15 wild-type sperm in triplicate dishes.

Collection of CD9-Containing Vesicles. The medium containing the vesicles was collected from denuded wild-type eggs. The eggs were cultured in a 60-μl drop of medium for 2 h after the zona pellucida was removed from the eggs. Collecting the medium containing the vesicles required an incubation time of 2 h. The collected medium was used for analysis of vesicle components and evaluation of sperm-fusing ability. CD9-depleted medium was used as a negative control. After the zona pellucida was removed from $CD9^{-/-}$ eggs, the eggs were incubated with the sperm in the medium containing CD9-incorporated vesicles for 1 h, for comparison with the vesicle-depleted medium. Details are shown in Fig. S3.

Western Blot Analysis. Quantities of proteins were examined by Western blot analysis, as described in ref. 4. As an internal loading control, quantities of albumin included in the medium were examined using Coomassie brilliant blue staining. Details are shown in Fig. S3.

Coincubation of Two Types of Eggs. $CD9^{-/-}$ eggs and CD9-expressing eggs ($CD9^{+/-}$ and $CD9^{+/+}$) were incubated in each 30-μl drop of medium after the zona pellucida was removed from these eggs. At 2 h after incubation, the $CD9^{-/-}$ eggs were added into the cultured medium of the CD9-expressing eggs. Sperm were added into the medium containing two types of eggs and incubated for 1 or 3 h. Details are shown in Fig. S4A. The frozen hamster eggs also were incubated with the $CD9^{-/-}$ eggs and wild-type sperm for 1 h. The zona pellucida of frozen hamster eggs was hardened, and removing the zona pellucida using acid Tyrode's solution took 5 min. Details are shown in Fig. S5A.

ACKNOWLEDGMENTS. This work was supported by a Precursory Research for Embryonic Science and Technology (PRESTO) grant from the Japanese Ministry of Health, Labor and Welfare and by a Grant-in-Aid for Scientific Research from the Japanese Ministry of Education, Culture, Sports, and Technology.

1. Yanagimachi R (1994) in *The Physiology of Reproduction*, eds Knobil E, Neill JD (Raven, New York), pp 189–317.
2. Kaji K, *et al.* (2000) The gamete fusion process is defective in eggs of Cd9-deficient mice. *Nat Genet* 24:279–282.
3. Le Naour F, Rubinstein E, Jasmin C, Prenant M, Boucheix C (2000) Severely reduced female fertility in CD9-deficient mice. *Science* 287:319–321.
4. Miyado K, *et al.* (2000) Requirement of CD9 on the egg plasma membrane for fertilization. *Science* 287:321–324.
5. Hemler ME (2003) Tetraspanin proteins mediate cellular penetration, invasion, and fusion events and define a novel type of membrane microdomain. *Annu Rev Cell Dev Biol* 19:397–422.
6. Barraud-Lange V, Naud-Barriant N, Bomsel M, Wolf J-P, Ziyyat A (2007) Transfer of oocyte membrane fragments to fertilizing spermatozoa. *FASEB J* 21:3446–3449.
7. Joly E, Hudrisier D (2003) What is trogocytosis and what is its purpose? *Nat Immunol* 4:815.
8. Runge K-E, *et al.* (2007) Oocyte CD9 is enriched on the microvillar membrane and required for normal microvillar shape and distribution. *Dev Biol* 304:317–325.
9. Traikovic K, *et al.* (2008) Ceramide triggers budding of exosome vesicles into multivesicular endosomes. *Science* 319:1244–1247.
10. Wubbolts R, *et al.* (2003) Proteomic and biochemical analyses of human B cell-derived exosomes: Potential implications for their function and multivesicular body formation. *J Biol Chem* 278:10963–10972.
11. Yamagata K, *et al.* (2002) Sperm from the calmegin-deficient mouse have normal abilities for binding and fusion to the egg plasma membrane. *Dev Biol* 250:348–357.
12. Mitsuzuka K, Handa K, Satoh M, Arai Y, Hakomori S (2005) A specific microdomain (''glycosynapse 3'') controls phenotypic conversion and reversion of bladder cancer cells through GM3-mediated interaction of alpha3beta1 integrin with CD9. *J Biol Chem* 280:35545–35553.
13. Yamashita T, *et al.* (2003) Enhanced insulin sensitivity in mice lacking ganglioside GM3. *Proc Natl Acad Sci USA* 100:3445–3449.
14. Kotani M, Ozawa H, Kawashima I, Ando S, Tai T (1992) Generation of one set of monoclonal antibodies specific for a-pathway ganglio-series gangliosides. *Biochim Biophys Acta* 1117:97–103.
15. Chen MS, *et al.* (1999) Role of the integrin-associated protein CD9 in binding between sperm ADAM 2 and the egg integrin alpha6beta1: Implications for murine fertilization. *Proc Natl Acad Sci USA* 96:11830–11835.
16. Miller B-J, Georges-Labouesse E, Primakoff P, Myles D-G (2000) Normal fertilization occurs with eggs lacking the integrin alpha6beta1 and is CD9-dependent. *J Cell Biol* 149:1289–1296.
17. Callahan M-K, Garg M, Srivastava P-K (2008) Heat-shock protein 90 associates with N-terminal extended peptides and is required for direct and indirect antigen presentation. *Proc Natl Acad Sci USA* 105:1662–1667.
18. Cheng M-Y, Hartl F-U, Horwich A-L (1990) The mitochondrial chaperonin hsp60 is required for its own assembly. *Nature* 348:455–458.
19. Bolte S, *et al.* (2004) FM-dyes as experimental probes for dissecting vesicle trafficking in living plant cells. *J Microsc* 214:159–173.
20. Yanagimachi R, Yanagimachi H, Rogers B-J (1976) The use of zona-free animal ova as a test system for the assessment of the fertilizing capacity of human spermatozoa. *Biol Reprod* 15:471–476.
21. Ponce R-H, Yanagimachi R, Urch U-A, Yamagata T, Ito M (1993) Retention of hamster oolemma fusibility with spermatozoa after various enzyme treatments: A search for the molecules involved in sperm–egg fusion. *Zygote* 1:163–171.
22. Primakoff P, Myles D-G (2002) Penetration, adhesion, and fusion in mammalian sperm–egg interaction. *Science* 296:2183–2185.
23. Booth A-M, *et al.* (2006) Exosomes and HIV *Gag* bud from endosome-like domains of the T cell plasma membrane. *J Cell Biol* 172:923–935.
24. Okada A, Yanagimachi R, Yanagimachi H (1986) Development of a cortical granule-free area of cortex and the perivitelline space in the hamster oocyte during maturation and following ovulation. *J Submicrosc Cytol* 18:233–247.
25. Zuccotti M, Yanagimachi R, Yanagimachi H (1991) The ability of hamster oolemma to fuse with spermatozoa: Its acquisition during oogenesis and loss after fertilization. *Development* 112:143–152.
26. Rankin T-L, *et al.* (1998) Human ZP3 restores fertility in Zp3 null mice without affecting order-specific sperm binding. *Development* 125:2415–2424.
27. Hogan B, Costantini F, Lacy E (1986) in *Manipulating the Mouse Embryo* (Cold Spring Harbor Lab Press, Cold Spring Harbor, NY), pp 217–252.
28. Toyoda Y, Chang M-C (1974) Capacitation of epididymal spermatozoa in a medium with high K-Na ratio and cyclic AMP for the fertilization of rat eggs in vitro. *J Reprod Fertil* 36:125–134.
29. Toshimori K, Saxena D-K, Tanii I, Yoshinaga K (1998) An MN9 antigenic molecule, equatorin, is required for successful sperm–oocyte fusion in mice. *Biol Reprod* 59:22–29.